



# EEG-based classification of Alzheimer's disease and frontotemporal dementia: a comprehensive analysis of discriminative features

Mehran Rostamikia<sup>1</sup> · Yashar Sarbaz<sup>1</sup> · Somaye Makouei<sup>1</sup>

Received: 24 March 2024 / Revised: 25 June 2024 / Accepted: 10 July 2024  
© The Author(s), under exclusive licence to Springer Nature B.V. 2024

## Abstract

Alzheimer's disease (AD) and frontotemporal dementia (FTD) are two main types of dementia. These diseases have similar symptoms, and they both may be considered as AD. Early detection of dementia and differential diagnosis between AD and FTD can lead to more effective management of the disease and contributes to the advancement of knowledge and potential treatments. In this approach, several features were extracted from electroencephalogram (EEG) signals of 36 subjects diagnosed with AD, 23 FTD subjects, and 29 healthy controls (HC). Mann–Whitney U-test and t-test methods were employed for the selection of the best discriminative features. The Fp1 channel for FTD patients exhibited the most significant differences compared to AD. In addition, connectivity features in the delta and alpha subbands indicated promising discrimination among these two groups. Moreover, for dementia diagnosis (AD + FTD vs. HC), central brain regions including Cz and Pz channels proved to be determining for the extracted features. Finally, four machine learning (ML) algorithms were utilized for the classification purpose. For differentiating between AD and FTD, and dementia diagnosis, an accuracy of 87.8% and 93.5% were achieved respectively, using the tenfold cross-validation technique and employing support vector machines (SVM) as the classifier.

**Keywords** Dementia-related diseases · EEG signal processing · Feature extraction · Feature selection · Diagnosis

## Introduction

Dementia is currently one of the greatest causes of death worldwide. It damages the brain and kills nerve cells, which usually results in a decline in cognitive function (Keene et al. 2001). Any cognitive impairment that is severe enough to interfere with independent, daily life activities is referred to as dementia. It is more accurate to define dementia as a syndrome than as a single illness (Gale et al. 2018). Dementia includes a wide range of diseases, and Alzheimer's disease (AD), Parkinson's

disease (PD) with dementia, dementia with Lewy bodies, and frontotemporal dementia (FTD) are some common and well-known examples of it (Wilson and Pagno 2019). There is evidence that by 2050, the number of people with dementia will be doubled worldwide (Scheltens et al. 2021), and AD, which is the most prevalent type of dementia, plays an important role in this statistical increase (Lane et al. 2017). Despite having made great progress in the field of diagnosis and preventing the advancement of AD, there is still no certain cure for AD, and treatment methods only control the symptoms (Briggs and Kennelly 2016). FTD is a less common form of dementia, and it includes changes in language, behavior, executive function, and motor symptoms (Olney et al. 2017). AD and FTD demonstrate similar symptoms in early stages. This usually leads to misdiagnosis or delay in diagnosis and difficulties in the treatment process as these two diseases are distinct neurodegenerative disorders with different progression patterns and causes. Thus, early detection of AD and FTD and differentiating these two has a significant impact on medical care, the life quality of patients, and professional

---

✉ Yashar Sarbaz  
yashar.sarbaz@tabrizu.ac.ir  
Mehran Rostamikia  
mehranrkia@gmail.com  
Somaye Makouei  
makouei@tabrizu.ac.ir

<sup>1</sup> Biomedical System Modeling Lab, Biomedical Engineering Department, Electrical and Computer Engineering Faculty, University of Tabriz, Tabriz, Iran

opportunities in their careers (Musa et al. 2020). Different methods can be implemented for diagnosing AD and FTD. Computed Tomography (CT) and Positron Emission Tomography (PET) are two imaging methods that are helpful in diagnosing AD (Wu et al. 2022), but they possess lower sensitivity in some cases compared to the functional Magnetic Resonance Imaging (fMRI) method (Ibrahim et al. 2021). For instance, fMRI-based studies showed different patterns of cortical thinning in AD and FTD, and AD patients showed thinner cortex in bilateral parietal and precuneus regions (Du et al. 2006). In another study (Yu et al. 2021) extracted the FTD and AD resemblance atrophy index, and the results showed the efficiency of MRI-based methods. The subset of machine learning methods based on artificial neural networks (deep learning methods), along with MRI-based differentiation, also result in high accuracy (Hu et al. 2021).

Electroencephalogram (EEG)-based studies (recording the electrical activity of the brain) also indicated high sensitivity for diagnosing neurodegenerative diseases in the resting state (Meghdadi et al. 2019). Extracting mean frequency, relative power, coherence, sample entropy, and multiscale entropy features from resting state EEG (the brain's on-going intrinsic activity) in PD and healthy control (HC) subjects and classifying them using Support Vector Machines (SVM) and convolutional neural networks (CNN) led to 88.88% and 98.66% accuracy, respectively (Yang et al. 2022). As well as PD, AD patients were distinguished from HC subjects with the implementation of resting state EEG signals in several studies. In some of these works, high accuracies were also achieved. EEG subbands power, which represents the amount of activity in certain frequency bands of the signal, was employed as the main feature in several articles (Rodrigues et al. 2018; Melissant et al. 2005; Huang et al. 2000; Lindau et al. 2003). Some of these studies used these features for diagnosing AD from HC, and an accuracy of 95%, 94%, and 84% was reached respectively, using different classification and feature selection strategies (Rodrigues et al. 2018; Melissant et al. 2005; Huang et al. 2000). AD appears to have an impact on these subbands' EEG power. Plenty of investigations have demonstrated that AD causes EEG signal power to increase at low frequencies and decrease at high frequencies (Melissant et al. 2005; Huang et al. 2000; Lindau et al. 2003; Nishida et al. 2011).

Many studies have tried to separate AD from FTD. One of the earliest studies in the field of diagnosis and differentiation of FTD and AD patients was done by (Lindau et al. 2003). They included a dataset of 19 FTD patients, 16 subjects diagnosed with AD, and 19 healthy individuals. Global field power (GFP, the overall strength of the electric field) of six frequency subbands ( $\delta, \theta, \alpha, \beta_1, \beta_2, \beta_3$ ) and the

ratio of the sum of fast frequency bands ( $\alpha, \beta_1, \beta_2, \beta_3$ ) and slow frequency bands ( $\delta, \theta$ ) were calculated as quantitative (qEEG) features. The Mann–Whitney U test was implemented as the statistical test for feature selection. The results showed different activity patterns in fast and slow frequency bands, and an accuracy of 93.3% was achieved. A study analyzed a dataset consisting of 19 AD, 19 FTD, and 21 HC subjects. The GFP of EEG frequency subbands was extracted, and standardized low-resolution electromagnetic tomography (sLORETA) was used to demonstrate the differences in brain functions between the three groups. Analysis of variance (ANOVA) and then post-hoc tests (identifying exactly which groups differ from each other) indicated that AD subjects have a higher GFP compared to HC in the delta frequency band, and in the alpha1 band, the GFP was higher in HC compared to FTD. The results also showed an increase in  $\beta_1$  GFP for FTD compared to AD, and 74% sensitivity was reached for classifying these two groups (Nishida et al. 2011). In another study, eight features were extracted, including mean, variance, the interquartile range (IQR), and the energy of five frequency bands for a dataset consisting of 10 AD, 10 FTD, and 8 control subjects. Six different machine learning algorithms classified these three groups, and two validation methods (tenfold cross-validation and leave-one-out validation) were used to validate the performance of the classifier. The outcome was 73% accuracy for differentiating AD and FTD using decision trees as classifier and leave-one-out as the validation method (Miltiadous et al. 2021). In another approach, a dataset consisted of 29 HC, 36 subjects diagnosed with AD, and 23 FTD patients were studied. Cross-frequency coupling, intra-frequency coupling, and graph features were extracted for five subbands, and the ANOVA test was used for feature selection. They concluded that AD indicates higher  $\delta$ – $\alpha$  and  $\delta$ – $\beta$  connectivity than the FTD, and 81.1% accuracy was achieved using Gaussian Naive Bayes (GNB) as the classifier (Si et al. 2023). Table 1 indicates the summary of previous studies' subject quantity, extracted features, classification method, and results.

Looking at the research done in the field of diagnosis and separation of AD, FTD, and HC, it is evident that the classification of AD and HC has been done with high accuracy in several studies. Unlike the classification of AD and HC, differentiating FTD from AD, has not yet been done with high precision. AD and FTD are two major subtypes of the dementia family, but the process of neuronal degeneration in these two diseases is different. Due to the similarity of these two diseases in the early stages in terms of symptoms, it is barely possible to determine the type of dementia exactly. In clinical processes, these two diseases are usually considered as dementia at first, and with the progress of the disease and the manifestation of other

**Table 1** Previous studies for the classification of AD, FTD, and HC

Authors	Subjects (HC, AD, FTD)	Extracted features	Classification
Huang et al. (2000)	24, 38	GFP	Linear discriminant
Lindau et al. (2003)	19, 16, 19	GFP and Spectral ratio	Logistic regression
Melissant et al. (2005)	31, 43	Independent component analyses (ICA) and subbands power	Feed-forward neural network, linear discriminant, k-nearest neighbors
Nishida et al. (2011)	22, 19, 19	GFP	sLORETA and ROC
Rodrigues et al. (2018)	11, 19	Subbands power, spectral ratios and number of minima, maxima and zero crossing	ANN
Miltiadous et al. (2021)	8, 10, 10	Mean, Variance, IQR, Energy	Decision trees Random forests
Si et al. (2023)	29, 36, 23	Phase Locking Value, graph features	GNB

symptoms specific to each disease, the treatment path for these two becomes different. If these two diseases can be diagnosed in the initial stage and then separated from each other, specific treatment can be applied in the early stages, and debilitating conditions can be postponed. In clinical diagnoses, there is a possibility of misdiagnosing the disease due to the lack of clarity in the symptoms of the disease in the early stages. The effect of these disorders, although insignificant, can be seen in the brain signals measured and displayed by the EEG signal. However, understanding the raw signal is difficult, and more processing should be done on the signal to identify insignificant alterations. Despite the fact that EEG subbands power seems to be the basis and discriminative characteristic for diagnosing neurological disorders, especially AD, it does not appear to be sufficient for separating AD from FTD. The majority of studies utilized EEG subbands power or other frequency-based features such as GFP, spectral ratio, and relative powers, and these features were not completely effective for this purpose. Moreover, in most of the studies, physiological disorders and variations in brain functions, particularly differences in EEG channels, have not been given enough attention. Improving the classification structure and making it two-stage, so that the disease is diagnosed first and then two different types of disease are separated, may lead to higher precision. Most of the previous studies have studied each disease compared to the normal subjects separately, and this may reduce the application of the works for clinical usages. In addition to the classification system, implementing a wider range of features, such as complex features and connectivity

patterns, which have not been paid attention to in differentiating between AD and FTD before, along with basic time-domain and frequency-domain features, might enhance the results. The current approach tries to provide a robust method and develop a comprehensive classification system that addresses the limitations of previous studies and analyzes the features related to each disorder in detail to provide a better understanding of the diseases.

## Materials and method

A summary of the proposed method in this study is illustrated in Fig. 1. This method consists of EEG recording, pre-processing, feature extraction, statistical analysis, and classification. Each part is described separately in the following sections.

### Dataset description

In this study, a publicly available dataset of 88 subjects was used (Miltiadous et al. 2023a, b, c). This dataset is conducted in accordance with the Declaration of Helsinki and approved by the Scientific and Ethics Committee of AHEPA University Hospital. The dataset includes the resting-state eyes-closed EEG of 29 HC, 23 subjects diagnosed with FTD, and 36 patients diagnosed with AD. The international Mini-Mental State Examination (MMSE) was used to evaluate the cognitive and neuropsychological status of subjects. A lower MMSE score indicates more severe cognitive impairment, and the MMSE score ranges

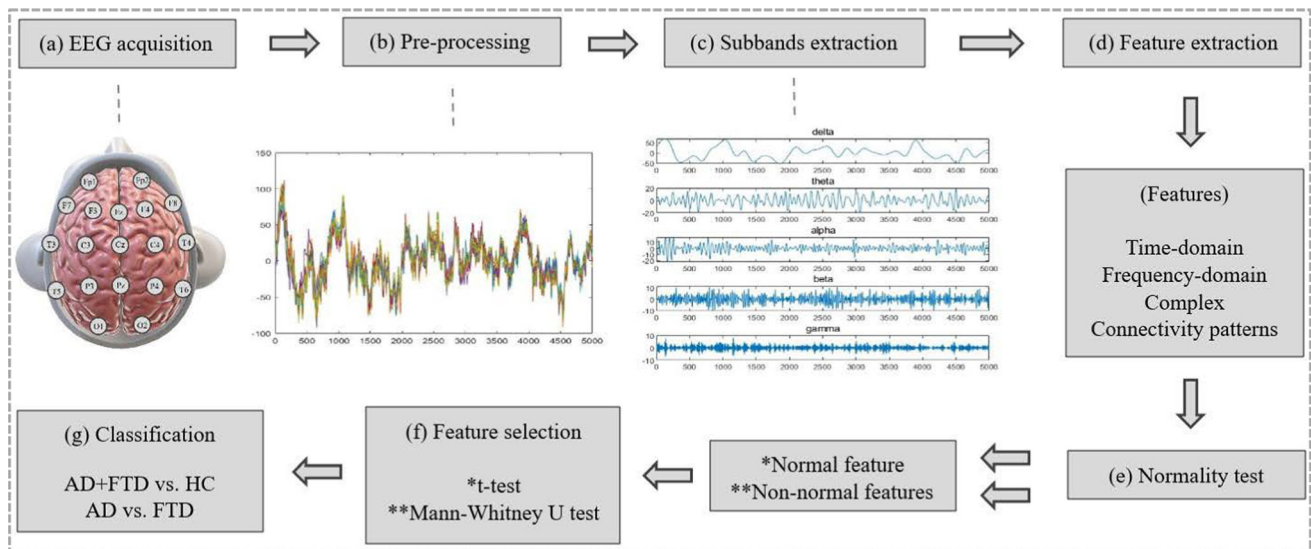


**Fig. 1** The schematic diagram of the proposed method for the classification of AD, FTD, and HC. This approach consists of seven main steps (a–g). The normality test in the (e) step divided the

features into two groups of normal and non-normal features, which are shown by \* and \*\* in the (f) step

from 0 to 30. The average MMSE score was 17.75 (SD = 4.5) for the AD group, 22.17 (SD = 8.22) for the FTD group, and 30 for the HC group. The median duration of disease measurement was 25 months, with the IQR range (Q1–Q3) being 24–28.5 months. No dementia-related coexisting conditions have been reported for patients. The average age was 66.4 (SD = 7.9) for the AD group, 67.9 (SD = 5.4) for the HC group, and 63.6 (SD = 8.2) for the FTD group.

The Nihon Kohden EEG 2100 clinical device was used for recording. Two reference electrodes (A1 and A2) were placed on the mastoids for the impedance check, and 19 scalp electrodes (Fp1, Fp2, F7, F3, Fz, F4, F8, T3, C3, Cz, C4, T4, T5, P3, Pz, P4, T6, O1, and O2) were implemented according to the 10–20 international system. 500 Hz of sampling at a resolution of 10uV/mm was utilized. With the Cz electrode as the common reference, the referential montage was performed. The parameters of the amplifier were as follows: Sensitivity: 10uV/mm, time constant: 0.3s, and high frequency filter at 70 Hz. The duration of each subject's EEG recording was approximately 13.5 min for the AD group (min = 5.1, max = 21.3), 12 min for the FTD group (min = 7.9, max = 16.9), and 13.8 min for the HC group (min = 12.5, max = 16.5). The dataset contains a total of 485.5 min of recording time for AD, 276.5 min for FTD, and 402 min for the HC group. Table 2 demonstrates the summarized information about subjects and EEG recordings.

## Pre-processing

The purpose of pre-processing was to remove noise and artifacts from the signals. The EEG recordings were pre-processed using the following steps: The raw EEG signals were in set format. The signals were re-referenced to A1–A2, and first a Butterworth band-pass filter (0.5–45 Hz), which is a signal processing filter designed to have a frequency response that is as flat as possible in the passband, was applied.

Next, the signals went through an application of the Artifact Subspace Reconstruction (ASR) routine, an EEG artifact correction technique that is part of the EEGLab Matlab software. ASR is a technique for cleaning EEG data by locating and eliminating artifact-contaminated segments. ASR begins by establishing baseline statistical properties through training on a clean segment of data. After that, it examines the data in brief windows, comparing each window's covariance to the baseline to look for artifacts. In order to effectively suppress noise and preserve the underlying neural signals, ASR reconstructs the affected segment by projecting it onto the subspace of the clean data when artifacts are detected. The method eliminated periods of bad data that exceeded the maximum allowable 0.5-s window standard deviation of 17. Then, the 19 EEG signals were converted to 19 ICA components using the Independent Component Analysis (ICA) method (RunICA program). ICA components that the EEGLAB platform's automatic classification process “ICLabel” categorized as “eye artifacts” or “jaw artifacts” were removed. In the final step, 250,000 middle samples (8.3 min approximately) of all subjects were saved to remove the possible

**Table 2** Dataset description

Group	Quantity	Gender male/female	Age (mean)	MMSE (mean)	EEG recording time (Each subject) (min)
HC	29	18/11	67.9	30	13.8
AD	36	12/24	66.4	17.75	13.5
FTD	23	14/9	63.6	22.17	12

The quantity, gender, and mean values of age, MMSE score, and recording time of each subject are illustrated

unwanted noises caused by patients' nervousness and exhaustion at the beginning and end of the signal recording. The following processes were done in the Matlab R2023b software on the output mat format file of each patient.

### Feature extraction

In this study, several features for all 19 channels of EEG recordings of all subjects were extracted. All features were selected based on the physiological changes that AD and FTD can cause to the electrical activity of the brain. The obtained features can be categorized into four groups: basic time-domain features, frequency-domain features, connectivity features, and complex features. The selected features are as follows:

#### Time-domain features

The time-domain features are considered fundamental characteristics in the EEG signals of neurological disorders. Extracting this type of feature is crucial to the quantification of the overall activity of the brain and the characterization of signal stability. These objectives can be achieved most effectively with the mean and variance features.

**Mean** In most cases of analyzing the EEG signals, the mean value of the EEG amplitude is considered a basic characteristic that can be different between the HC, AD, and FTD subjects based on their neurological differences. The mean value for each channel was calculated using the following formula:

$$\bar{x} = \frac{1}{N} \sum_{i=1}^N x_i, \quad i = 1, 2, 3, \dots, N \quad (1)$$

where  $x$  is each EEG channel's signal and  $N$  is the signal's length.

**Variance** The second basic time-domain feature that was calculated is variance, which is the measurement of the amount of spread in a signal. Neurological disorders may cause a significant difference in the distribution of a signal's amplitude around the mean value. Variance was achieved using the following formula:

$$\sigma^2 = \frac{1}{N} \sum_{i=1}^N (x_i - \bar{x})^2, \quad i = 1, 2, 3, \dots, N \quad (2)$$

where  $\bar{x}$  is the mean value.

#### Frequency-domain features

Interpreting the time-domain raw EEG signals is difficult. Each frequency subband in the electrical activity of the brain is associated with specific neural processes and cognitive functions. EEG signals can be separated into a number of specific frequency subbands to analyze the activity of the brain related to specific tasks at those corresponding frequencies. For this purpose, subbands power was calculated to assess the total alterations in each subband. Furthermore, the total power of five frequency subbands can be a practical feature for evaluating the overall activity of the brain in different regions. As illustrated in Table 1, these features were also used in several studies to detect neurological disorders. Also, frequency-domain features proved to be practical in diagnosing other diseases like epilepsy (Guerrero et al. 2021), and mild cognitive impairment in PD (Liu et al. 2023). EEG is a non-stationary signal, which means it changes over time. In non-stationary signals, the discrete wavelet transform (DWT) can be used to extract features in time–frequency analysis, and it has many advantages compared to the short-time Fourier transform (STFT) (Bajaj 2021). Thus, DWT with the 4th order Daubechies (db4) serving as the mother wavelet was implemented to decompose the EEG signals into five frequency subbands of delta ( $\delta = .5$ –4 Hz), theta ( $\theta = 4$ –8 Hz), alpha ( $\alpha = 8$ –14 Hz), beta ( $\beta = 14$ –30 Hz), and gamma ( $\gamma = 30$ –45 Hz). Next, the following features were obtained for all five subbands.

**Subbands power** The EEG subband power indicates the amount of activity within specific frequency subbands. The brain has specific activities in a particular frequency subband, and neurodegenerative diseases, such as AD, in a person can cause defects in the functioning of the brain at certain subbands (Al-Qazzaz et al. 2014). Therefore, each subband's power was obtained using the following procedure:



First, the signal went through the Fast Fourier Transform (fft), which was determined by:

$$F_i = |\text{fft}(x_i)|^2 \quad (3)$$

and using the following formula, the trapezoidal area of the signal was obtained:

$$\text{Power}_j = \int_a^b F_i dF \quad (4)$$

where  $j = \delta, \theta, \alpha, \beta, \gamma$  subbands.  $a$  and  $b$  are the signal's length.

**Total Power** The sum of the signal power at all five subbands of the EEG signals is used to obtain this feature.

$$\text{Total Power} = \sum_{i=\delta}^{\gamma} \text{Power}_i, i = \delta, \theta, \alpha, \beta, \gamma \quad (5)$$

### Connectivity patterns

Connectivity features measure the functional connection between different brain regions. The brain is a complex system, and this system has various components that interact with each other. Neurological disorders alter the parameters of this system and cause differences in those interactions. One of the best methods to investigate these interactions and observe their changes in patients is to use the EEG signal. Different EEG channels are placed in different parts of the brain, making it possible to compare the interaction of these areas in healthy people and patients by extracting connectivity features. Several studies analyzed the connectivity patterns in other diseases and achieved good results (Peláez Suárez et al. 2021; Dickinson et al. 2021). AD and FTD cause abnormalities in brain functioning and coordination of various activities. Cross-correlation and coherence are two fundamental features for assessing both frequency-specific and time-specific connectivity in neurological disorders and the communication of different brain regions.

**Cross-correlation** The similarity between EEG electrodes can be measured by the cross-correlation feature. It measures the similarity by shifting one signal in time on the lagged version of the other one. The cross-correlation of 19 EEG channels was measured using the following steps:

First, the cross-covariance for two signals of  $y_{1,t}$ ,  $y_{2,t}$  and lags of  $k = 0, \pm 1, \pm 2, \dots$  was achieved by:

$$C_{y_1 y_2}(k) = \begin{cases} \frac{1}{T} \sum_{t=1}^{T-k} (y_{1,t} - \bar{y}_1)(y_{2,t+k} - \bar{y}_2); k=0, 1, 2, \dots \\ \frac{1}{T} \sum_{t=1}^{T+k} (y_{2,t} - \bar{y}_2)(y_{1,t-k} - \bar{y}_1); k=0, -1, -2, \dots \end{cases} \quad (6)$$

where  $\bar{y}_1$  and  $\bar{y}_2$  are the sample means of selected channels' data. Next, the sample standard deviations were estimated by:

$$\begin{aligned} S_{y_1} &= \sqrt{C_{y_1 y_1}(0)} \text{ where } C_{y_1 y_1}(0) = \text{Var}(y_1), S_{y_2} \\ &= \sqrt{C_{y_2 y_2}(0)}, \text{ where } C_{y_2 y_2}(0) = \text{Var}(y_2) \end{aligned} \quad (7)$$

Finally, Cross-Correlation was estimated by:

$$r_{y_1 y_2}(k) = \frac{C_{y_1 y_2}(k)}{S_{y_1} S_{y_2}}, k = 0, \pm 1, \pm 2, \dots \quad (8)$$

The maximum value of the cross-correlation coefficients was stored as the main characteristic. This process was done for each pair of electrodes, and a total of 171 features were extracted for each subject. For all five subbands, cross-correlation was extracted for further detailed analysis of brain connections at different frequencies.

**Coherence** This feature computes the coherence between each pair of EEG channels in the frequency domain. To evaluate the degree of synchronization between signals at various frequency components, coherence analysis is often used. Through the identification of specific connection patterns related to particular disorders, coherence analysis can facilitate the process of differential diagnosis (Shaw 1981). For each pair of EEG electrodes, coherence was obtained employing the following formula:

$$C_{xy}(f) = \frac{|P_{xy}(f)|^2}{P_{xx}(f)P_{yy}(f)} \quad (9)$$

where  $P_{xx}(f)$  and  $P_{yy}(f)$  are power spectral densities, and  $P_{xy}(f)$  is the cross power spectral density of a given pair of signals. The mean value of the coherence signal was picked as the main feature. For a more detailed examination of the coherence and dynamic changes across different brain states, this feature was also extracted at five frequency bands.

### Complex features

EEG signals may contain certain patterns that are not easily discernible. The brain has a dynamic structure, and neurological diseases change the dynamic state of the brain. These changes are different in each dynamical state and were investigated in other diseases like PD and epilepsy (Garehdaghi and Sarbaz 2023; Fiorenzato et al. 2023; Özçelik and Altan 2023). Complex features can be useful in resolving this issue. In this study, three types of complex

features were extracted. The selection of these features was done in a way that extract the dynamic properties in the best way possible.

**Katz fractal dimension (KFD)** The human's brain contains regularity and a fractal nature in its electrical activity. The fractal dimension of time-series data can be estimated using the KFD method. It is especially useful for analyzing temporal signals to determine their complexity and regularity, such as EEG signals (Raghavendra et al. 2009). KFD was estimated using the following steps:

First,  $L$  is calculated that is the total length of the curve, which is the sum of the Euclidean distances (Britannica 2023) between successive points in the signal. Then,  $d$  which is the Euclidean distance between the first point of the sequence and each subsequent point (i.e., diameter of the waveform) is estimated and the maximum distance was stored. Finally, KFD was obtained using the following formula:

$$KFD = \frac{\log_{10} n}{\log_{10}(n) + \log_{10}(d/L)} \quad (10)$$

where  $n$  is the number of steps in the waveform.

**Lyapunov Exponents (LE)** The chaotic behavior and complexity of the electrical activity in the brain can be studied using LE (Barreira 2017). This feature measures the rate of divergence of nearby trajectories in a dynamical system, and a higher value of LE indicates a more complex and chaotic system. Neurodegenerative diseases can reduce the LE value, which can be used for diagnostic purposes. LE was estimated by the following algorithm:

First, a delayed reconstruction  $Y_{1:N}$  with embedding dimension  $m$  and lag  $\tau$  was generated. Then, for a point  $i$ , nearest neighbor point  $i^*$  was found in a way that satisfies  $i^* \text{Min} \|Y_i - Y_{i^*}\|$ . Next, the Lyapunov exponent for the entire expansion range, which is the range of initial conditions over which the trajectories of a dynamical system exhibit exponential divergence, was calculated by:

$$\lambda(i) = \frac{1}{(K_{max} - K_{min} + 1)dt} \sum_{K=K_{min}}^{K_{max}} \frac{1}{k} \ln \frac{\|Y_{i+k} - Y_{i^*+k}\|}{\|Y_i - Y_{i^*}\|} \quad (11)$$

where,  $K_{max}$  and  $K_{min}$  are expansion ranges.

**Approximate Entropy (ApEn):** The amount of irregularity or complexity of a signal can be measured by ApEn (Delgado-Bonal et al. 2019). The likelihood that identical patterns of data points will remain the same when the dimensions of the patterns (the embedding dimension) are increased by one is compared. This offers us a way to characterize the complexity of the EEG signals by analyzing the consistency of patterns within the time series. ApEn was estimated by taking the following steps:

First, a delayed reconstruction  $Y_{1:N}$ , for  $N$  data points with embedding dimension  $m$ , and lag  $\tau$  was created. Then, the number of within range points, at point  $i$ , obtained by:

$$N_i = \sum_{k=1, k \neq i}^N d(\|Y_i - Y_k\|_{\infty} < R) \quad (12)$$

where,  $d$  is the indicator function, and  $R$  is the radius of similarity. Finally, ApEn was given by:

$$\varphi_m = (N - m + 1)^{-1} \sum_{i=1}^{N-m+1} \log(N_i) \quad (13)$$

$$ApEn = \varphi_m - \varphi_{m+1} \quad (14)$$

## Statistical analysis

In this study, statistical analysis was implemented to choose the most significant features for two-group differentiation. First, the Kolmogorov–Smirnov test was applied to verify the normal distribution of extracted features for each channel. A  $p$ -value of 0.05 was selected as the distribution's normality threshold. The features that met the normality test were evaluated for significant difference between two groups using the t-test method. Features with a non-normal distribution were assessed by the Mann–Whitney U test. Features with a  $p$ -value less than 0.05 were considered as the discriminative features. This process was done in two separate steps. First, AD and FTD patients were combined to create the dementia group. Thus, the dementia group was compared with the HC group. Then, the AD and FTD groups were analyzed to differentiate the two diseases. In this method, multiple comparisons were omitted, and only two groups were examined in each step.

## Classification

In this approach, the first step was to consider AD and FTD as a single group to be compared with the HC group. In the second step, AD and FTD were differentiated. The purpose of this method is to identify the type of dementia after making an initial diagnosis of the illness. All of the discriminative features with their  $p$ -value less than 0.05 served as the train and test data for the classification. 70% of the participants were used for training, and the remaining 30% were used to test the classifier's performance. Furthermore, the tenfold cross-validation method was employed to prevent classifier overfitting.

Four machine learning (ML) algorithms were employed for classification. Support vector machines (SVM) with gaussian and linear kernels, k-nearest neighbor (KNN), Naive Bayes (NB), and random forest (RF) served as classifiers. The selection criteria for these algorithms were

their popularity and application in the classification of neurological diseases in previous studies (Melissant et al. 2005; Miltiadous et al. 2021; Najafzadeh et al. 2021; Si et al. 2023). The accuracy, sensitivity, and specificity of the system were estimated using the following formulas:

$$\text{Accuracy} = \frac{TP + TN}{TP + TN + FP + FN} \quad (15)$$

$$\text{Sensitivity} = \frac{TP}{TP + FN} \quad (16)$$

$$\text{Specificity} = \frac{TN}{TN + FP} \quad (17)$$

where TP is true positive, TN is true negative, FP is false positive, and FN is false negative results. Table 3 represents the classifiers and the chosen hyper-parameters.

## Results

For all participants' EEG signal recordings, four types of time-domain, frequency-domain, connectivity patterns, and complex features were extracted for all EEG channels. Then, statistical analysis was employed to pick the most discriminative features for two classification processes. The first classification case was for dementia diagnosis (AD + FTD vs. HC), and then the second classifier was employed for differentiating between AD and FTD patients.

Table 4 demonstrates the classification accuracy, sensitivity, and specificity obtained by employing four ML algorithms. As illustrated in Table 4, the best classification accuracy was obtained using the SVM classifier. For differentiating between AD and FTD, an accuracy of 87.8% was achieved, and for dementia diagnosis, an accuracy of 93.5% was reached.

**Table 3** Classifiers' hyper-parameters

Classifier	Hyper-parameters	
	AD + FTD vs. HC	AD vs. FTD
SVM	Linear kernel	Gaussian kernel
	Auto scale	Auto scale
	Box constraint = 3	Box constraint = 1
	Kernel offset = 2	Kernel offset = 1
KNN	K = 4	K = 4
	Distance metric: Euclidean	Distance metric: Minkowski
NB	Distributions: kernel	Distributions: kernel
RF	Number of trees: 100	Number of trees: 150

Best results achieved using these parameters. Hyper-parameters are illustrated for each classifier separately

In the case of diagnosing dementia, numerous channels exhibited significant differences. Figure 2 demonstrates the most significant channels and the number of discriminative features in each channel. Connectivity features are not taken into account in Fig. 2 to consider the characteristics specific to each brain area, and the pairs of EEG electrodes do not play a role in this figure. Furthermore, the mean value and standard deviation (SD) of the most discriminative time-domain, frequency-domain, complex, and connectivity features is illustrated in Fig. 3.

For differentiating between AD and FTD patients, several features exhibited significant variations in specific channels. Figure 4 demonstrates the most discriminative time-domain, frequency-domain, complex, and connectivity features and their mean and SD values for all subjects in the AD and FTD groups. Also, for a more detailed analysis of differences between these two diseases, EEG couplings with the highest differences in their coherence and cross-correlation features in their relevant subbands are illustrated in Figs. 5 and 6, respectively. Tables 5 and 6 represent the *p*-values related to the most discriminative features for dementia diagnosis and differentiating between two diseases, respectively.

The best results for differentiating between AD and FTD were obtained when features with *p*-values of 0.05 or lower were utilized, and for the purpose of classifying participants into patients and normal subjects, features with *p*-values of 0.005 or lower were considered. Furthermore, the results of each iteration (each training and testing) of the tenfold cross-validation technique using the SVM classifier are shown in Fig. 7. The comparison of the results of previous works with the current study can be seen in Table 7.

## Discussion

In this study, the EEG-based classification of AD, FTD, and HC was done in a detailed and thorough way. Each step was performed in a way that covered the defects and limitations of previous studies. The following explanations provide a complete outlook on the importance of the current study, comprehensive methodology, and a clinical view of the achieved results.

Neurodegenerative diseases can cause neuron loss in the brain and, in most cases, lead to dementia-related disorders. AD is the most prevalent form of dementia, which affects memory, behavior, thinking, and even body movements in the final stages (Kurlan et al. 2000; Förstl et al. 1999). In the early stages of AD, the hippocampus gets affected (De Leon et al. 1989). This area is important for memory formation, and AD causes the destruction of brain cells in this structure (Rao et al. 2022). With the progression of the



**Table 4** Classification accuracy, sensitivity, and specificity for AD vs. FTD and AD + FTD vs. HC

Classifier	AD vs. FTD			AD + FTD vs. HC		
	Accuracy (%)	Sensitivity (%)	Specificity (%)	Accuracy (%)	Sensitivity (%)	Specificity (%)
SVM	<b>87.8</b>	85.1	<b>90.0</b>	<b>93.5</b>	<b>90.0</b>	<b>93.0</b>
KNN	83.5	<b>90.0</b>	83.3	87.7	80.4	90.5
NB	85.5	75.0	88.3	81.5	85.0	77.5
RF	85.5	80.5	88.6	86.6	75.5	93.0

These results were obtained using formulas in the 2.5 section

The highest-obtained results were shown in the bold format

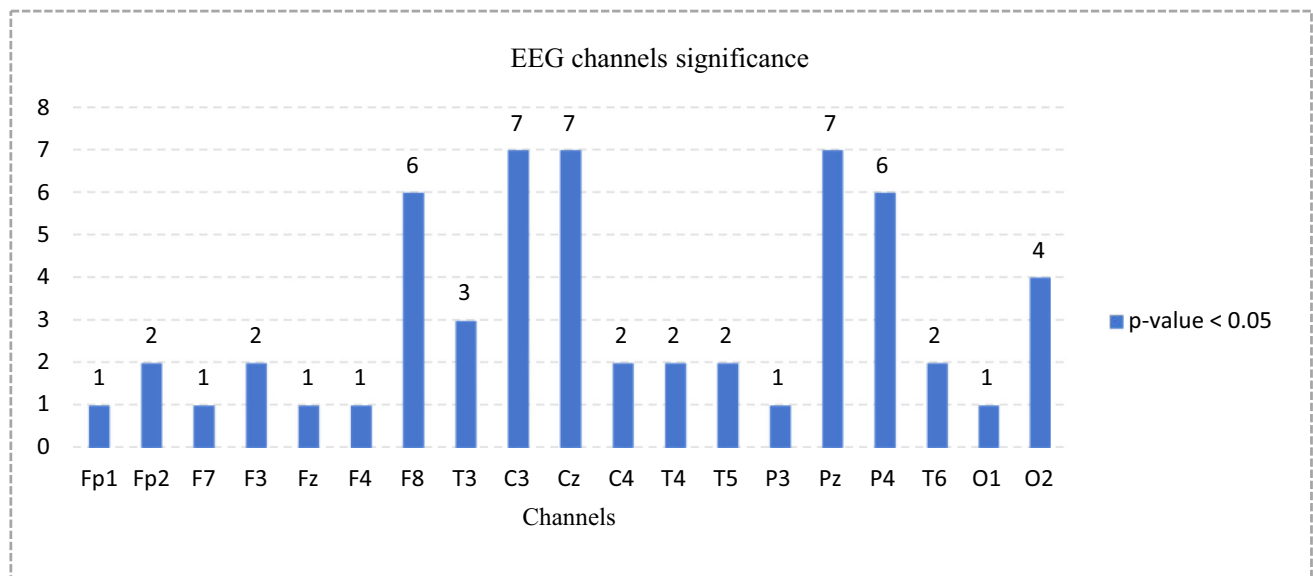


**Fig. 2** EEG channels with the most disparities among AD + FTD and HC groups. The number of features with their  $p$ -values < 0.05 are indicated in each channel

disease, other parts of the brain get damaged, and at the last stages, AD can spread all over the brain, leading to severe cognitive impairment (Kraemer et al. 1998). FTD is another type of dementia that mainly affects language, behavior, and personality in the early stages and as the disease progresses, it causes memory loss (Mioshi et al. 2010). The frontal and temporal lobes of the brain, which are responsible for executive functions, decision-making, language, and processing of auditory and visual information, get affected by FTD. As well as AD, FTD impacts other regions of the brain with the advancement of the disease (Rosen et al. 2002). There is no specific treatment method for AD and FTD, and existing approaches can only cure the symptoms of the disease (Briggs and Kennelly 2016). AD and FTD exhibit similar symptoms in the early stages; however, progression patterns and symptoms vary for each disease. Also, the existing methods of controlling the progress of AD and FTD differ, and the medications for

each group are distinct (Rascovsky et al. 2005; Du et al. 2006). As a result, differentiating between AD and FTD and early diagnosis of dementia is crucial, and it can help the affected person control the disease progression and provide better treatment methods that can prevent some dementia-related conditions from getting worse. EEG is an effective tool for detecting the electrical activity of the brain. Resting-state EEG has many advantages over other methods of diagnosing brain disorders. It has high temporal resolution, is low-cost, and does not include any invasive procedures. Additionally, portable EEG devices can be utilized, and they are suitable for patients with difficulties in their movement.

In this study, several features were extracted from the resting-state eyes-closed EEG recordings of 29 HC subjects, 23 FTD subjects, and 36 subjects diagnosed with AD. The mean and variance were extracted as the basic time-domain features of the EEG signals. These two features

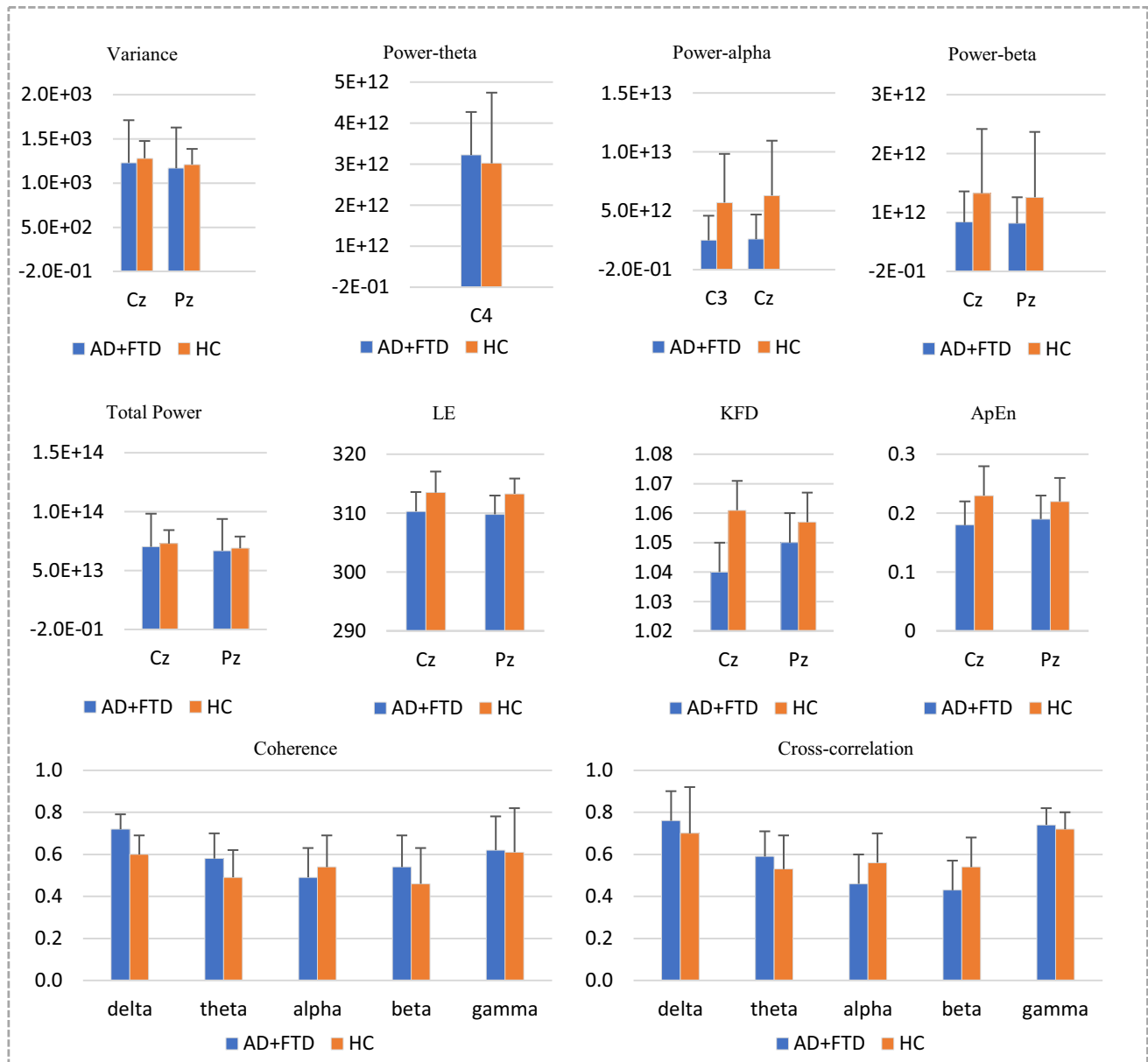


**Fig. 3** The mean and SD values of the most discriminative features for dementia diagnosis. The Y axis in each shape illustrates the amounts obtained by each feature. Also, the corresponding channels and subbands are shown below each column

provided us with an elementary outlook on the overall activity of the brain in patients and normal subjects. The power of the EEG signals for five frequency subbands and the total power were obtained as the frequency-domain features. As the frequency-based features were obtained in the five frequency subbands, each of those features indicated differences related to specific dynamics of the brain that are altered because of the disease. For more detailed analyses of dynamical changes in the brain, complex (time–frequency) features were obtained. For this purpose, KFD, LE, and ApEn features were calculated. These complex features enabled us to examine the dynamical

changes from three different angles. Finally, the cross-correlation and the coherence were extracted for detecting the connectivity patterns of different brain regions. These two connectivity features allowed us to investigate the interactions of different brain regions in the time and frequency domains. The aim of this study was to diagnose dementia at the first step and then differentiate between AD and FTD groups. Thus, the AD and FTD patients were combined and considered as the dementia group to be compared with the HC group. Then, two groups of the AD and FTD were compared to differentiate those subjects. The normal distribution of features was assessed using the

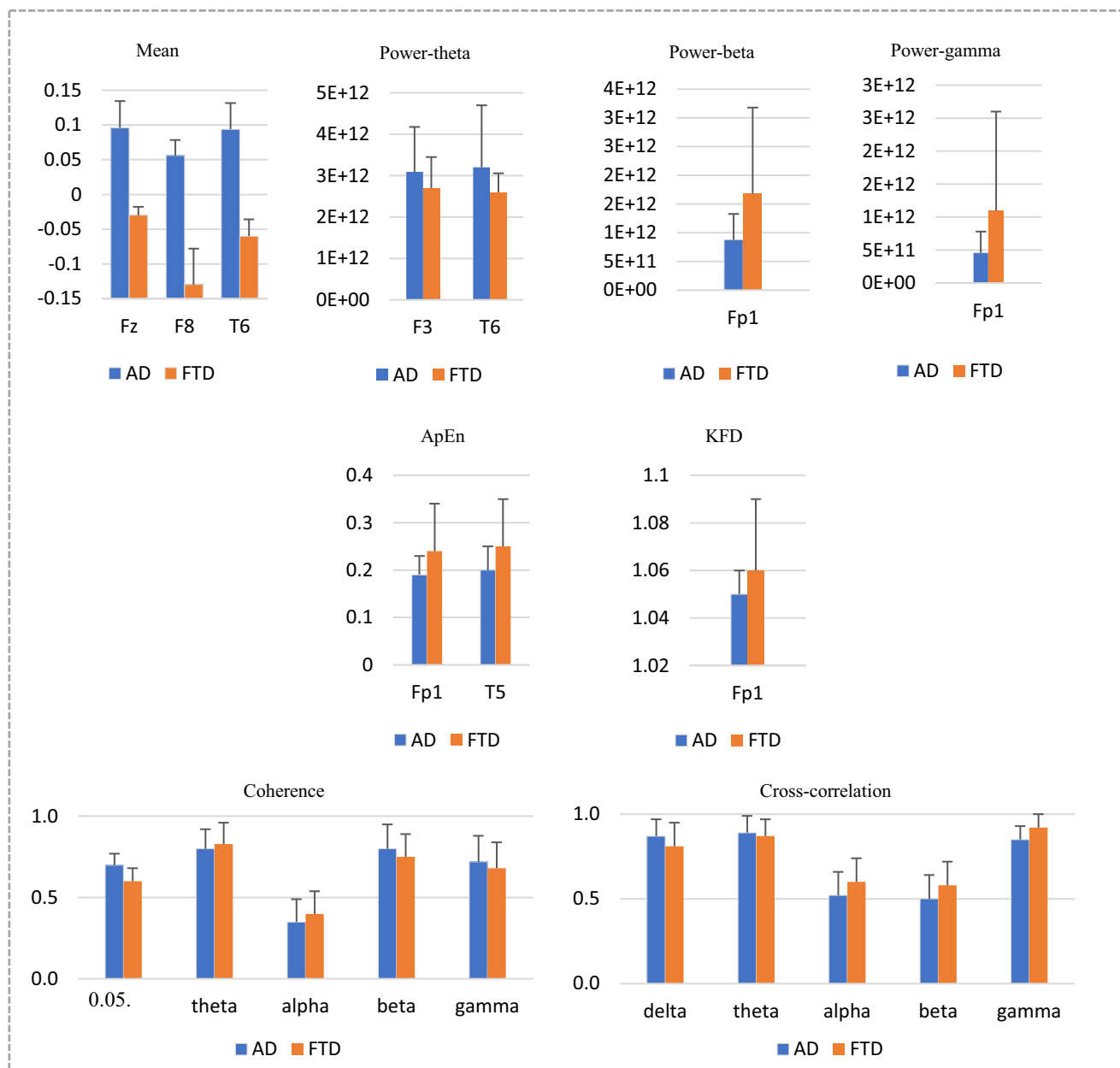


**Fig. 4** The mean and SD values of the most discriminative features for differentiating AD and FTD patients. The Y axis in each shape illustrates the amounts obtained by each feature. Also, the corresponding channels and subbands are shown below each column

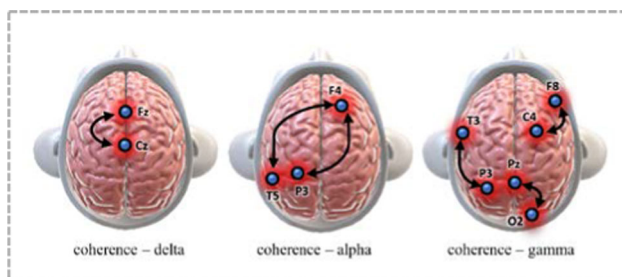


**Fig. 5** EEG couplings with the highest differences between AD and FTD patients for the coherence feature

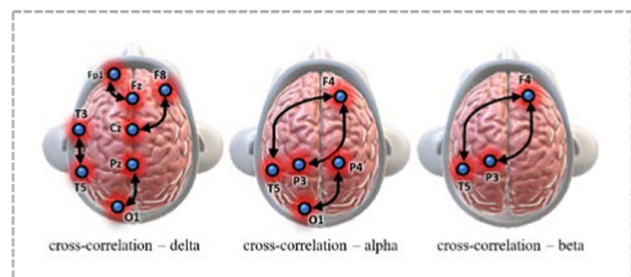


**Fig. 6** EEG couplings with the highest differences between AD and FTD patients for the cross-correlation feature

**Table 5** For dementia diagnosis, the most significant channels in each feature and the corresponding *p*-values are illustrated

Feature	Channels	Subbands	<i>p</i> -value
Variance	Cz, Pz	–	0.01, 0.004
Power-theta	C4	–	0.01
Power-alpha	C3, Cz	–	< 0.0001, < 0.0001
Power-beta	Cz, Pz	–	< 0.0001, < 0.0001
Total power	Cz, Pz	–	0.005, 0.001
LE	Cz, Pz	–	< 0.0001, < 0.0001
KFD	Cz, Pz	–	< 0.0001, 0.003
ApEn	Cz, Pz	–	0.0001, 0.01
Coherence	–	$\delta, \theta, \alpha, \beta, \gamma$	0.001, 0.03, 0.002, 0.005, 0.0001
Cross-correlation	–	$\delta, \theta, \alpha, \beta, \gamma$	0.0003, 0.001, 0.001, 0.03, 0.002

The *p*-values for connectivity features are the mean values of couplings with their *p*-value less than 0.05

**Table 6** For differential diagnosis of two diseases, the most significant channels in each feature and the corresponding *p*-values are illustrated

Authors	Classification groups	Results
Huang et al. (2000)	AD vs. HC	84% Accuracy
Lindau et al. (2003)	AD vs. FTD	93.3% Accuracy
Melissant et al. (2005)	AD vs. HC	94% Accuracy
Nishida et al. (2011)	AD vs. FTD	74% Sensitivity
	AD vs. HC	74% Sensitivity
	FTD vs. HC	55% Sensitivity
Rodrigues et al. (2018)	AD vs. HC	95% Accuracy
Miltiadous et al. (2021)	AD vs. FTD	73% Accuracy
	AD vs. HC	78.5% Accuracy
	FTD vs. HC	86.3% Accuracy
Si et al. (2023)	AD vs. FTD	81.1% Accuracy
Proposed method	AD + FTD vs. HC	93.5% Accuracy
	AD vs. FTD	87.8% Accuracy

The *p*-values for connectivity features are the mean values of couplings with their *p*-value less than 0.05. The *p*-values marked with \* indicate that there were no significant couplings

Kolmogorov–Smirnov test, and statistical analysis was implemented for feature reduction. The Mann–Whitney U test method for non-normally distributed features and the t-test method for normally distributed features were employed for this purpose.

As illustrated in Figs. 2 and 3, the most discriminative channels for dementia diagnosis were Cz and Pz, which are the midline central and parietal regions in the brain. In addition, as displayed in Fig. 4, the Fp1 channel played the most important role in differentiating between AD and FTD. The results proved that with the gradual loss of neurons, the variability of the electrical activity of the brain in AD patients significantly decreases compared to the HC

and FTD groups. Although the overall variance values for patients with dementia declined compared to the HC group, FTD and HC subjects exhibited similar variance values in several channels. These results suggest that, with the gradual development of the disease and the loss of neurons, the brain's ability to produce many different kinds of patterns of activity decreases as fewer neurons are available to participate in the electrical activity. The mean values in AD patients showed a significant rise in Fz, F8, and T6 channels compared to FTD patients. These channels correspond to the frontal and temporal regions, respectively, which get affected mainly in FTD patients, and as a result, fewer EEG values are seen in this group. The subbands power also exhibited significant differences in both cases of dementia diagnosis and differentiation of the two diseases. In the slow-frequency activities, particularly in the theta subband, which is related to memory functions and processes, AD patients revealed a significant increase compared to the FTD group in the frontal and temporal brain regions. These regions are more affected by FTD than AD, and the results prove the defection of slow-frequency activities in the FTD group. Likewise, in the central brain regions, patients with dementia showed an increase in theta subband power compared to the HC group. These increases in patients can be caused by the dysfunctionality of neurons, resulting in a compensatory mechanism in specific brain regions. In the fast-frequency subbands, which are associated with cognitive functions, there is a direct relationship between neurons degeneration and a reduction in power values. As a result, patients with dementia demonstrated a decrease in alpha and beta subbands, particularly in C3, Cz, and Pz channels. Also, in the beta and gamma subbands, the FTD group exhibited a significant power increase compared to the AD group in the Fp1 channel. The cognitive processes of attention, working memory, and higher-order cognitive processing are all related to the beta and gamma frequency bands. The Fp1 channel power increase seen in these

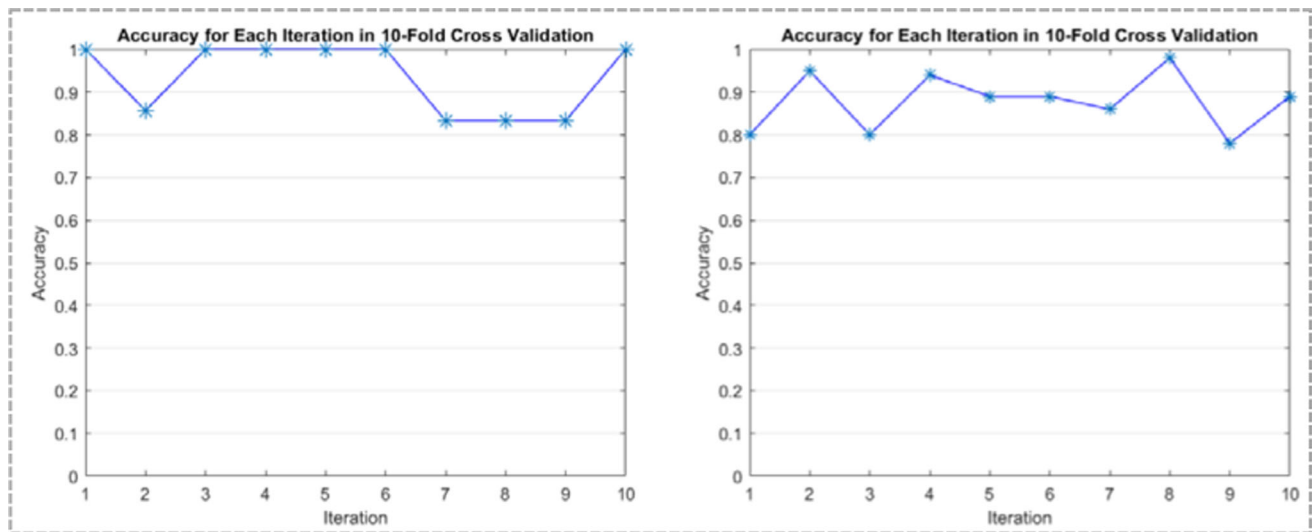


**Fig. 7** The results of ten-time iteration for dementia diagnosis (left) and differential diagnosis (right). The mean and SD of the tenfold cross validation are  $87.8\% \pm 6.4\%$  for differential diagnosis and

$93.5\% \pm 7.8\%$  for dementia diagnosis using the SVM classifier. The images are obtained from Matlab R2023b software

**Table 7** The comparison of the results achieved by previous studies and the current methodology

Feature	Channels	Subbands	<i>p</i> -value
Mean	Fz, F8, T6	–	0.003, 0.02, 0.01
Power-theta	F3, T6	–	0.03, 0.04
Power-beta	Fp1	–	0.01
Power-gamma	Fp1	–	0.01
ApEn	Fp1, T5	–	0.04, 0.02
KFD	Fp1	–	0.04
Coherence	–	$\delta, \theta, \alpha, \beta, \gamma$	0.03, 0.05 < *, 0.02, 0.05 < *, 0.02
Cross-correlation	–	$\delta, \theta, \alpha, \beta, \gamma$	0.03, 0.05 < *, 0.005, 0.01, 0.05 < *

frequency bands in FTD patients may be a sign of compensatory changes in neural activity associated with these cognitive functions. The total power of five frequency bands also indicated a direct relationship with the progression of disease, and the HC group depicted higher power values compared to AD and FTD. Also, there was a slight difference between the AD and FTD groups in total power values, and patients with AD showed a negligible increase compared to the FTD group. For the LE feature, the HC group showed significantly higher values compared to the AD and FTD groups in all EEG channels. The most discriminative channels were the Cz and Pz electrodes. This determines the more chaotic behavior of the brain in normal subjects compared to dementia-related diseases, and as the disease progresses, the brain functions more randomly. The LE values for AD and FTD patients were approximately the same, and there were only small differences. This suggests that the overall dynamical complexity of brain activity is altered with the onset of disease, and the type of dementia is does not determine the amount of chaotic behavior in the brain. The ApEn and KFD

features also exhibited promising results in both cases. The results showed that with the advancement of the disease and the affection of more brain areas, irregular oscillations in electrical activity decreased. That means the obtained values for ApEn and KFD were significantly higher in patients with dementia than in the HC group. Furthermore, patients with AD exhibited a significant drop in both ApEn and KFD values compared to the FTD group in the Fp1 and T5 channels. These findings prove the existence of more complex and irregular patterns in normal subjects, and with the progression of disease, the EEG signals indicate more regular behavior. Connectivity patterns also proved to be discriminative in several subbands. The mean values of coherence for patients with AD significantly increased in the delta subband and decreased in the theta and alpha subbands compared to the FTD group. As illustrated in Fig. 5, the most discriminative couplings were in the frontal-central, frontal-parietal, and temporal-parietal areas. The cross-correlation feature was also beneficial for differentiating between AD and FTD. Frontal-parietal, frontal-temporal, and frontal-central couplings showed the



major differences between these two groups, as shown in Fig. 6. The cross-correlation of EEG channels in AD groups exhibited a significant increase in the delta subband and a decrease in the alpha and beta subbands compared to the FTD group. For dementia diagnosis, the most discriminative subbands in coherence and cross-correlation features were the delta, alpha, and gamma subbands, and features with the lowest  $p$ -values were seen in these subbands. In both coherence and cross-correlation features, there was a significant increase in the delta and gamma subbands and a decrease in the alpha subband in patients diagnosed with dementia. Frontal–temporal couplings in the delta subband and temporal–temporal couplings in the alpha and gamma subbands exhibited the most differentiation between patients and normal subjects. These changes in brain couplings reflect the neuropathological changes in the mentioned subbands and regions and variations in communication among different brain areas due to disorders in the cognitive and memory systems.

In this study, we tried to examine several features in specific brain areas to find the alterations in different brain regions that these features revealed. Overall, a number of channels proved to be determining in diagnosing the disease and the differentiation of two dementia subgroups. For dementia diagnosis, the Cz and Pz channels exhibited notable differences and can be considered the basic regions in which most alterations occur. The Cz electrode is placed over the cortex and mainly detects electrical activities associated with attention and cognitive control processes. Moreover, the Pz electrode is placed over the parietal lobe, which mainly contributes to episodic memory retrieval, visuospatial processing, and attentional processing. From the results given by the extracted features, it can be observed that there is a significant decrease in Cz and Pz channels' variance, power in alpha and beta subbands, total power, ApEn, KFD, and LE feature values. Furthermore, couplings with these channels played a crucial role in connectivity patterns in particular subbands. It can be concluded that dementia mostly affects brain areas in connection with the mentioned channels, and these effects are more noticeable in the form of a decrease compared to the HC group in various features due to the disruption of brain functions. For the purpose of differentiating the two diseases, Fp1 and several temporal channels showed the most significant variations among these two groups. The Fp1 channel, which tracks the brain's left prefrontal lobe activities, is mostly associated with language processing and executive functions. This channel exhibited the most variations between AD and FTD patients. Patients diagnosed with FTD mainly exhibited higher values in the power of beta and gamma subbands, ApEn, KFD, and connectivity patterns in the alpha subband. As a result, the Fp1 channel plays a key role in the separation of AD and

FTD. To ensure the performance and usefulness of the extracted features and the obtained results, several classifiers were employed. For dementia diagnosis, 93.5% accuracy was achieved, and for differentiating AD and FTD patients, 87.8% accuracy was reached, which approved the efficiency of the proposed method. The obtained result for differentiating AD and FTD is considerably more accurate than the previous works done in this field. As it can be seen in Table 7, our result in the classification of two diseases is mostly higher than previous studies which had 74% sensitivity, 73%, and 81.1% accuracy (Nishida et al. 2011; Miltiadous et al. 2021; Si et al. 2023). Also, dementia diagnosis was barely studied in previous works, but we can claim that our result in this case is very proper, considering that two subgroups were combined, and this made the classification process more challenging than one group versus one group study cases in previous works (Nishida et al. 2011; Rodrigues et al. 2018; Miltiadous et al. 2021).

There were limitations in this work that can be considered as perspectives for future works. One of the limitations of this study was the small population of the applied dataset. Although the preliminary results were satisfactory, the generalizability of these findings cannot be assured. The total number of subjects present in this study was 88, and in order to generalize the results, studies on a much larger population should be conducted. Also, the current study suffered from gender biases that should be avoided as much as possible. Moreover, the population of three subgroups was not equal, and this may cause errors for the classifiers. A more comprehensive dataset with a much greater population, including different stages of the diseases without biases, can lead to robust results. The use of a 19-channel EEG signal can cause limitations in recording the electrical activity of different parts of the brain. For more accurate recording, EEG devices with more channels can be used. Also, in future works, different subgroups of dementia can be compared with each other.

Diagnosing neurological diseases is crucial for the treatment and control process, and usually the diagnosis of subgroups of diseases from a family is mistaken. One of these diseases is dementia the differential diagnosis of its two subtypes, FTD and AD, is problematic. In this work, we tried to carefully separate them according to the dynamics of the brain and the effects that diseases have on the brain. The features that were used, deal with the dynamic structure and how the brain communicates with each other. Finally, the SVM machine learning method, which is a powerful classifier, was used and was able to differentiate diseases with high accuracy. The remarks in this article were that first, people with dementia were placed in a group and were compared with healthy people. Then, two disorders were compared with each other, and

this is the power of our work that can be used in practice. Satisfactory results were also obtained (87.8% and 93.5% for differential and dementia diagnosis, respectively), and it can be used as a comprehensive method for the classification of AD, FTD, and HC subjects. It is hoped that the investigated method can be used in other diseases and their differential diagnosis and draw conclusions.

**Acknowledgements** We acknowledge Andreas Miltiadous and his team for data collection and making it publicly available to researchers in OpenNeuro website (Miltiadous et al. 2023a, b).

**Funding** No external funding was received.

**Data availability** The data that support the findings of this study are openly available in OpenNeuro website at <https://openneuro.org/datasets/ds004504>.

## Declarations

**Conflict of interest** All authors contributed equally and have approved the final manuscript. None of the authors have potential conflicts of interest to be disclosed.

**Ethical approval** All experimental procedures and protocols was conducted in accordance with the Declaration of Helsinki and approved by the Scientific and Ethics Committee of AHEPA University Hospital, Aristotle University of Thessaloniki, under protocol number 142/12-04-2023.

## References

- Al-Qazzaz NK, Shbmd A, Ahmad SA, Chellappan K, Islam MdS, Escudero J (2014) Role of EEG as biomarker in the early detection and classification of dementia. *Sci World J* 2014:1–16. <https://doi.org/10.1155/2014/906038>
- Bajaj N (2021) Wavelets for EEG analysis. *Wavelet Theory*. <https://doi.org/10.5772/intechopen.94398>
- Barreira L (2017) Lyapunov exponents and regularity. *Lyapunov Exp* 2017:31–41. [https://doi.org/10.1007/978-3-319-71261-1\\_2](https://doi.org/10.1007/978-3-319-71261-1_2)
- Briggs R, Kennelly SP, O'Neill D (2016) Drug treatments in Alzheimer's disease. *Clin Med* 16:247–253. <https://doi.org/10.7861/clinmedicine.16-3-247>
- Britannica T (2023) Editors of Encyclopaedia Euclidean space. *Encyclopedia Britannica*. <https://www.britannica.com/science/Euclidean-space>
- De Leon M, George A, Stylopoulos L, Smith G, Miller D (1989) Early marker for Alzheimer's disease: the atrophic hippocampus. *Lancet* 334:672–673. [https://doi.org/10.1016/s0140-6736\(89\)90911-2](https://doi.org/10.1016/s0140-6736(89)90911-2)
- Delgado-Bonal A, Marshak A (2019) Approximate entropy and sample entropy: a comprehensive tutorial. *Entropy* 21:541. <https://doi.org/10.3390/e21060541>
- Dickinson A, Daniel M, Marin A, Gaonkar B, Dapretto M, McDonald NM, Jeste S (2021) Multivariate neural connectivity patterns in early infancy predict later autism symptoms. *Biol Psychiatry Cogn Neurosci Neuroimag* 6:59–69. <https://doi.org/10.1016/j.bpsc.2020.06.003>
- Du A-T, Schuff N, Kramer JH, Rosen HJ, Gorno-Tempini ML, Rankin K, Miller BL, Weiner MW (2006) Different regional patterns of cortical thinning in Alzheimer's disease and frontotemporal dementia. *Brain* 130:1159–1166. <https://doi.org/10.1093/brain/awm016>
- Fiorenzato E, Moaveninejad S, Weis L, Biundo R, Antonini A, Porcaro C (2023) Brain dynamics complexity as a signature of cognitive decline in Parkinson's disease. *Mov Disord* 39:305–317. <https://doi.org/10.1002/mds.29678>
- Förstl H, Kurz A (1999) Clinical features of Alzheimer's disease. *Eur Arch Psychiatry Clin Neurosci* 249:288–290. <https://doi.org/10.1007/s004060050101>
- Gale SA, Acar D, Daffner KR (2018) Dementia. *Am J Med* 2018(131):1161–1169. <https://doi.org/10.1016/j.amjmed.2018.01.022>
- Garehdaghi F, Sarbaz Y (2023) Analyzing global features of magnetic resonance images in widespread neurodegenerative diseases: new hope to understand brain mechanism and robust neurodegenerative disease diagnosis. *Med Biol Eng Comput* 61:773–784. <https://doi.org/10.1007/s11517-022-02748-0>
- Guerrero L-D, Romero LD, Bueno-Lopez M (2021) A review of epileptic seizure detection using EEG signals analysis in the time and frequency domain. In: 2021 IEEE 21st international conference on communication technology (ICCT). <https://doi.org/10.1109/ICCT52962.2021.9657835>
- Hu J, Qing Z, Liu R, Zhang X, Lv P, Wang M, Wang Y, He K, Gao Y, Zhang B (2021) Deep learning-based classification and voxel-based visualization of frontotemporal dementia and Alzheimer's disease. *Front Neurosci* 14:626154. <https://doi.org/10.3389/fnins.2020.626154>
- Huang C, Wahlund L-O, Dierks T, Julin P, Winblad B, Jelic V (2000) Discrimination of Alzheimer's disease and mild cognitive impairment by equivalent EEG sources: a cross-sectional and longitudinal study. *Clin Neurophysiol* 111:1961–1967. [https://doi.org/10.1016/s1388-2457\(00\)00454-5](https://doi.org/10.1016/s1388-2457(00)00454-5)
- Ibrahim B, Suppiah S, Ibrahim N, Mohamad M, Hassan HA, Nasser NS, Saripan MI (2021) Diagnostic power of resting-state fMRI for detection of network connectivity in Alzheimer's disease and mild cognitive impairment: a systematic review. *Hum Brain Mapp* 42:2941–2968. <https://doi.org/10.1002/hbm.25369>
- Keene J, Hope T, Fairburn CG, Jacoby R (2001) Death and dementia. *Int J Geriatr Psychiatry* 16:969–974. <https://doi.org/10.1002/gps.474>
- Kraemer HC, Taylor JL, Tinklenberg JR, Yesavage JA (1998) The stages of Alzheimer's disease: a reappraisal. *Dement Geriatr Cogn Disord* 9:299–308. <https://doi.org/10.1159/000017081>
- Kurlan R, Richard IH, Papka M, Marshall F (2000) Movement disorders in Alzheimer's disease: More rigidity of definitions is needed. *Mov Disord* 15:24–29. [https://doi.org/10.1002/1531-8257\(200001\)15:1%3c24::aid-mds1006%3e3.0.co;2-x](https://doi.org/10.1002/1531-8257(200001)15:1%3c24::aid-mds1006%3e3.0.co;2-x)
- Lane CA, Hardy J, Schott JM (2017) Alzheimer's disease. *Eur J Neurol* 2017(25):59–70. <https://doi.org/10.1111/ene.13439>
- Lindau M, Jelic V, Johansson S-E, Andersen C, Wahlund L-O, Almkvist O (2003) Quantitative EEG abnormalities and cognitive dysfunctions in frontotemporal dementia and Alzheimer's disease. *Dement Geriatr Cogn Disord* 15:106–114. <https://doi.org/10.1159/000067973>
- Liu C, Jiang Z, Liu S, Chu C, Wang J, Liu W, Sun Y, Dong M, Shi Q, Huang P, Zhu X (2023) Frequency-dependent microstate characteristics for mild cognitive impairment in Parkinson's disease. *IEEE Trans Neural Syst Rehab Eng* 31:4115–4124. <https://doi.org/10.1109/TNSRE.2023.3324343>
- Meghdadi AH, Karic MS, Berka C (2019) EEG analytics: benefits and challenges of data driven EEG biomarkers for neurodegenerative diseases. In: 2019 IEEE international conference on systems, man and cybernetics (SMC). <https://doi.org/10.1109/smc.2019.8914065>
- Melissant C, Ypma A, Frietman EEE, Stam CJ (2005) A method for detection of Alzheimer's disease using ICA-enhanced EEG

- measurements. *Artif Intell Med* 33:209–222. <https://doi.org/10.1016/j.artmed.2004.07.003>
- Miltiados A, Tzamourta KD, Giannakeas N, Tsiouras MG, Afrantou T, Ioannidis P, Tzallas A (2021) Alzheimer's disease and frontotemporal dementia: a robust classification method of EEG signals and a comparison of validation methods. *Diagnostics* 11:1437. <https://doi.org/10.3390/diagnostics11081437>
- Miltiados A, Gionanidis E, Tzamourta KD, Giannakeas N, Tzallas AT (2023a) DICE-Net: a novel convolution-transformer architecture for Alzheimer detection in EEG signals. *IEEE Access* 11:71840–71858. <https://doi.org/10.1109/ACCESS.2023.3294618>
- Miltiados A, Tzamourta KD, Afrantou T, Ioannidis P, Grigoriadis N, Tsalikakis DG, Angelidis P, Tsiouras MG, Glavas E, Giannakeas N, Tzallas AT (2023b) A dataset of 88 EEG recordings from: Alzheimer's disease, Frontotemporal dementia and Healthy subjects. 10.18112/OPENNEURO.DS004504.V1.0.5
- Miltiados A, Tzamourta KD, Afrantou T, Ioannidis P, Grigoriadis N, Tsalikakis DG, Angelidis P, Tsiouras MG, Glavas E, Giannakeas N, Tzallas AT (2023c) A dataset of scalp EEG recordings of Alzheimer's disease, frontotemporal dementia and healthy subjects from routine EEG. *Data* 8:95. <https://doi.org/10.3390/data8060095>
- Mioshi E, Hsieh S, Savage S, Hornberger M, Hodges JR (2010) Clinical staging and disease progression in frontotemporal dementia. *Neurology* 74:1591–1597. <https://doi.org/10.1212/wnl.0b013e3181e04070>
- Musa G, Slachevsky A, Muñoz-Neira C, Méndez-Orellana C, Villagra R, González-Billault C, Ibáñez A, Hornberger M, Lillo P (2020) Alzheimer's disease or behavioral variant frontotemporal dementia: review of key points toward an accurate clinical and neuropsychological diagnosis. *JAD* 73:833–848. <https://doi.org/10.3233/jad-190924>
- Najafzadeh H, Esmaili M, Farhang S, Sarbaz Y, Rasta SH (2021) Automatic classification of schizophrenia patients using resting-state EEG signals. *Phys Eng Sci Med* 44:855–870. <https://doi.org/10.1007/s13246-021-01038-7>
- Nishida K, Yoshimura M, Isotani T, Yoshida T, Kitaura Y, Saito A, Mii H, Kato M, Takekita Y, Suwa A, Morita S, Kinoshita T (2011) Differences in quantitative EEG between frontotemporal dementia and Alzheimer's disease as revealed by LORETA. *Clin Neurophysiol* 122:1718–1725. <https://doi.org/10.1016/j.clinph.2011.02.011>
- Olney NT, Spina S, Miller BL (2017) Frontotemporal dementia. *Neurol Clin* 2017(35):339–374. <https://doi.org/10.1016/j.ncl.2017.01.008>
- Özçelik YB, Altan A (2023) A comparative analysis of artificial intelligence optimization algorithms for the selection of entropy-based features in the early detection of epileptic seizures. In: 2023 14th international conference on electrical and electronics engineering (ELECO). <https://doi.org/10.1109/ELECO60389.2023.10415957>
- Peláez Suárez AA, Berrillo Batista S, Pedrosa Ibáñez I, Casabona Fernández E, Fuentes Campos M, Chacón LM (2021) EEG-derived functional connectivity patterns associated with mild cognitive impairment in Parkinson's disease. *Behav Sci* 11:40. <https://doi.org/10.3390/bs11030040>
- Raghavendra BS, Narayana Dutt D (2009) A note on fractal dimensions of biomedical waveforms. *Comput Biol Med* 39:1006–1012. <https://doi.org/10.1016/j.combiomed.2009.08.001>
- Rao YL, Ganaraja B, Murlimanju BV, Joy T, Krishnamurthy A, Agrawal A (2022) Hippocampus and its involvement in Alzheimer's disease: a review. *3 Biotech* 12:55. <https://doi.org/10.1007/s13205-022-03123-4>
- Rascovsky K, Salmon DP, Lipton AM, Leverenz JB, DeCarli C, Jagust WJ, Clark CM, Mendez MF, Tang-Wai DF, Graff-Radford NR, Galasko D (2005) Rate of progression differs in frontotemporal dementia and Alzheimer disease. *Neurology* 65:397–403. <https://doi.org/10.1212/01.wnl.0000171343.43314.6e>
- Rodrigues PM, Freitas DR, Teixeira JP, Alves D, Garrett C (2018) Electroencephalogram signal analysis in Alzheimer's disease early detection. *Int J Reliab Q E-Healthc* 7:40–59. <https://doi.org/10.4018/ijrqeh.2018010104>
- Rosen HJ, Gorno-Tempini ML, Goldman WP, Perry RJ, Schuff N, Weiner M, Feiwell R, Kramer JH, Miller BL (2002) Patterns of brain atrophy in frontotemporal dementia and semantic dementia. *Neurology* 58:198–208. <https://doi.org/10.1212/wnl.58.2.198>
- Scheltens P, De Strooper B, Kivipelto M, Holstege H, Chételat G, Teunissen CE, Cummings J, van der Flier WM (2021) Alzheimer's disease. *Lancet* 2021(397):1577–1590. [https://doi.org/10.1016/s0140-6736\(20\)32205-4](https://doi.org/10.1016/s0140-6736(20)32205-4)
- Shaw JC (1981) An introduction to the coherence function and its use in EEG signal analysis. *J Med Eng Technol* 5:279–288. <https://doi.org/10.3109/03091908109009362>
- Si Y, He R, Jiang L, Yao D, Zhang H, Xu P, Ma X, Yu L, Li F (2023) Differentiating between Alzheimer's disease and frontotemporal dementia based on the resting-state multilayer EEG network. *IEEE Trans Neural Syst Rehabil Eng* 31:4521–4527. <https://doi.org/10.1109/tnsre.2023.3329174>
- Wilson H, Pagano G, Politis M (2019) Dementia spectrum disorders: lessons learnt from decades with PET research. *J Neural Transm* 126:233–251. <https://doi.org/10.1007/s00702-019-01975-4>
- Wu H, Lei Z, Ou Y, Shi X, Xu Q, Shi K, Ding J, Zhao Q, Wang X, Cai X, Liu X, Lou J, Liu X (2022) Computed tomography density and  $\beta$ -amyloid deposition of intraorbital optic nerve may assist in diagnosing mild cognitive impairment and Alzheimer's disease: a 18F-flutemetamol positron emission tomography/computed tomography study. *Front Aging Neurosci* 2022:14. <https://doi.org/10.3389/fnagi.2022.836568>
- Yang C-Y, Huang Y-Z (2022) Parkinson's disease classification using machine learning approaches and resting-state EEG. *J Med Biol Eng* 42:263–270. <https://doi.org/10.1007/s40846-022-00695-7>
- Yu Q, Mai Y, Ruan Y, Luo Y, Zhao L, Fang W, Cao Z, Li Y, Liao W, Xiao S, Mok VCT, Shi L, Liu J (2021) An MRI-based strategy for differentiation of frontotemporal dementia and Alzheimer's disease. *Alzheimer Res Therapy* 2021:13. <https://doi.org/10.1186/s13195-020-00757-5>

**Publisher's Note** Springer Nature remains neutral with regard to jurisdictional claims in published maps and institutional affiliations.

Springer Nature or its licensor (e.g. a society or other partner) holds exclusive rights to this article under a publishing agreement with the author(s) or other rightsholder(s); author self-archiving of the accepted manuscript version of this article is solely governed by the terms of such publishing agreement and applicable law.